Monatsh Chem (2013) 144:495–500
DOI 10.1007/s00706-012-0881-7

ORIGINAL PAPER

Boronic acid-based autoligation of nucleic acids: influence of the nature of the 3′-end ribonucleotidic strand

Renaud Barbeyron · Jesper Wengel · Jean-Jacques Vasseur · Michael Smietana

Received: 28 September 2012 / Accepted: 13 November 2012 / Published online: 14 December 2012
© Springer-Verlag Wien 2012

Abstract The development of synthetic systems displaying dynamic and adaptive characteristics is a formidable challenge with wide applications from biotechnology to therapeutics. Recently, we described a dynamic and programmable nucleic acid-based system relying on the formation of reversible boronate internucleosidic linkages. The DNA- or RNA-templated system comprises a 5′-ended boronic acid probe connecting a 3′-ended ribonucleosidic oligonucleotide partner. To explore the dominant factors that control the reversible linkage, we synthesized a series of 3′-end modified ribonucleotidic strands. Evidence suggests that geometric and steric factors are key features for controlling the equilibria.

Keywords Boron · Complexation · DNA · Dynamic processes · Template synthesis

Introduction

The transfer of genetic information undoubtedly relies on selection, amplification, and correction processes. It is now widely accepted that these processes are the outcome of simple chemical systems that evolved into functional self-organized architectures [1, 2]. One of the many issues scientists face concerning the structure of contemporary nucleic acids is the selection of phosphodiester internucleosidic linkages [3]. Indeed, non-enzymatic synthesis of oligonucleotides from simple building blocks requires phosphate activation, which often leads to mixtures of compounds [4–7]. To overcome these problems, non-enzymatic DNA- and RNA-templated ligation systems displaying high ligation fidelity have been developed. Relying on the hybridization of two half-length oligomers along a template, many ligation chemistries have been used to generate natural or modified backbones [8–18]. While remarkable, these systems lack the adaptive and corrective parameters necessary for the genetic polymers to evolve. In turn, it has been suggested that these parameters could be achieved using reversible linkages able to respond to external stimuli [19–24]. In this context, we recently developed a dynamic DNA- and RNA-templated ligation system based on the reversible formation of cyclic five-membered boronate internucleosidic linkages. The ligation that does not require any added reagent occurs through the reaction of two half-stranded probes, one carrying a boronic acid at its 5′-end, while its partner would feature a natural 3′-end ribonucleotide (Fig. 1). We also demonstrated that the system displayed adaptative behavior responding to external stimuli such as temperature, pH, diol concentration, and cyanide ions [25–28]. In order to explore the factors that influence the sensitivity and stability of the boronate internucleosidic linkage, we surveyed its formation by varying the nature of the 3′-end ribonucleotidic strand. We report here our investigation aimed at delineating the optimum structural features that drive the dynamic system.

R. Barbeyron · J.-J. Vasseur · M. Smietana (✉)
Institut des Biomolécules Max Mousseron, UMR 5247
CNRS-Université Montpellier 1, Université Montpellier, 2,
place Eugène Bataillon, 34095 Montpellier, France
e-mail: msmietana@um2.fr

J. Wengel
Nucleic Acid Center, Department of Physics,
Chemistry and Pharmacy, University of Southern Denmark,
Campusvej 55, 5230 Odense M, Denmark

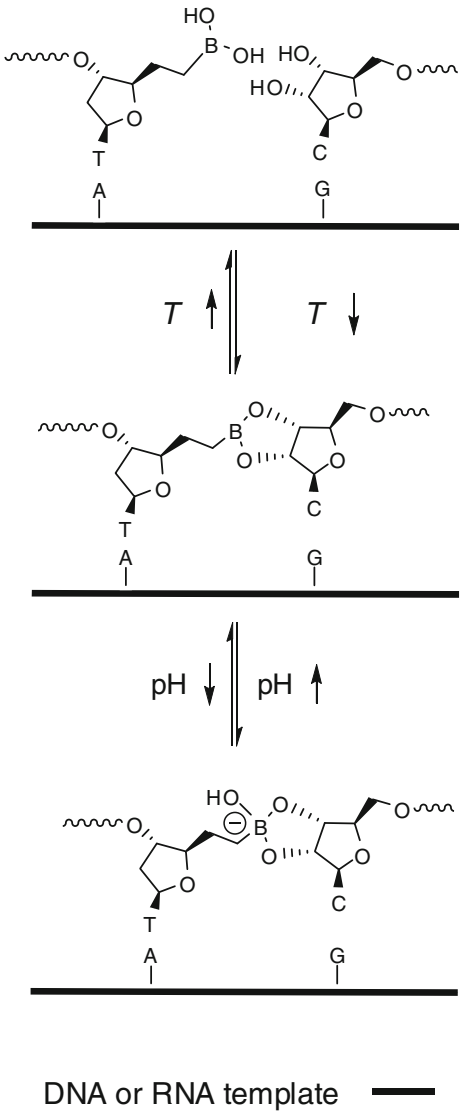

Fig. 1 Mechanism of the boronic acid-based autoligation process resulting in boronate ester

Results and Discussion

It is well known that boronic acids react reversibly with 1,2- and 1,3-substituted Lewis base donors and particularly cis-diol groups to form boronic esters [29, 30]. The overall process is an equilibrium that can be shifted by azeotropic distillation of the water or with the use of a dehydrating agent. In water, the formation of a diol boronate complex can be favored at high pH as a consequence of a rehybridation of the boronic ester (neutral trigonal boron, *sp*2 hybridized) to a hydroxy boronate ester (anionic tetrahedral boron, *sp*3 hybridized) [31, 32]. At neutral pH simple Lewis bases such as fluoride [33–35] and cyanide ions are also known to trigger the formation of *sp*3 species [36]. These properties have notably been used for the development of boronic acid-based sensors [29, 34, 37, 38]. However, many issues could affect the boronic acid/diol complexation. For the diol moiety, it has been demonstrated that low pK_A values, small O–C–C–O dihedral angles, steric hindrance, and restricted rotations around the C–C bond of the diol are key factors for optimal binding [29, 32, 39].

Associated with structural restrictions imposed by the double helix, it is crucial to understand the intrinsic preference that governs the boronic acid-based DNA-templated autoligation process.

The series of 3′-end sequences investigated is shown in Fig. 2. Along with natural uridine (**1**), we probed conformational, electronic, chemical, and optimal spacing features of the hybridizing probes. Derivatives **2** and **3** were selected to evaluate two contrasted flexible and rigid modifications. Aminonucleosides **4** and **5** were chosen for their ability to trigger the formation of oxazaborolidines along the template. Finally, to investigate the effects of relative positions of hybridization, we synthesized sequences in which bases were deleted (compound **6** and **7a**) or had an added cis-diol motif (compound **7b**).

Our experimental design involves a 14mer DNA- or RNA-template (ODN**D** and ORN**R** respectively), a 5′-boronic acid heptathymidinylate sequence (ODN**B**), and the 3′-end modified sequences ODN**X**. The two half-stranded probes exhibit purposefully major differences in affinity for the complementary strand (Table 1, entries 1 and 2; T_m = 14.8 °C for ODN**D**/ODN**B** and T_m = 38.7 °C for ODN**D**/ODN**1**). Control experiments carried out with $(dT)_7$ (ODN**C**), an analog of ODN**B** without the boronic acid modification, are given for comparison. All curves featured a double sigmoidal transition corresponding to the transition of the half-duplexes with the template. Our goal was to explore whether the templated ligation between ODN**B** and ODN**X** could occur and to what extent. Since the boronic acid functionality is carried by the less stable half-duplex, the formation of a novel boronate-linked full duplex mainly influences the lower transition. Considering that the boronate/diol complex could be stabilized at high pH, we first probed the pH effect on the different systems. Results are presented in Table 1. As expected, ODN**1** triggered the autoligation at pH 7.5, leading to a boronate-ligated duplex having a melting temperature 6.1 °C higher than that of the nicked dsDNA (T_m = 20.9 vs. 14.8 °C, Table 1, entry 3). This stabilization goes up to 16.0 °C at pH = 9.5 (T_m = 30.8 vs. 14.8 °C, Table 1, entry 3) as a consequence of the rehybridation of boron from *sp*2 to *sp*3. In contrast, ODN**2**, which features an acyclic RNA mimic lacking a bond between the C2′ and C3′ atoms of the ribose ring, was unable to induce the autoligation irrespective of the pH of the experiments (Table 1, entry 4). Despite the destabilization of duplexes generally induced by acyclic nucleosides, it has been demonstrated that Watson-Crick

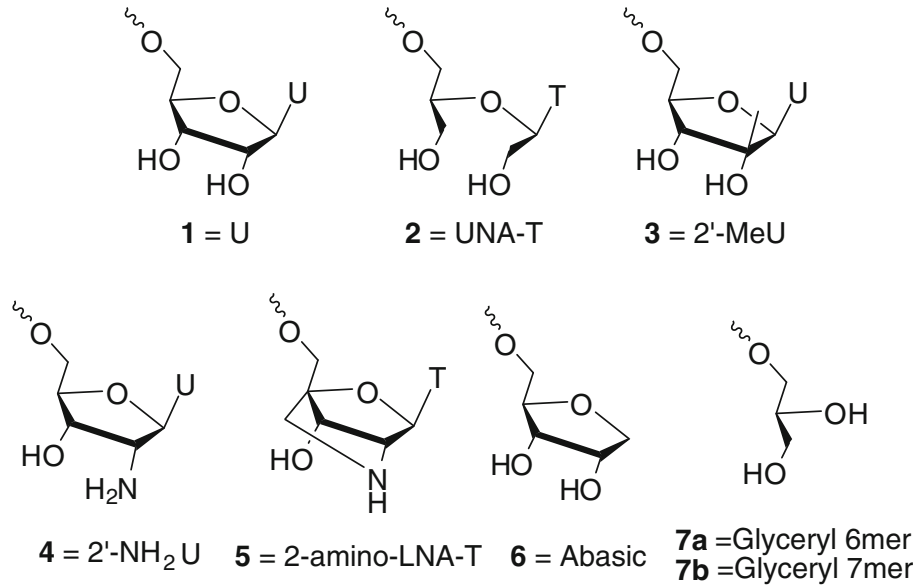

Fig. 2 Structures of sequences considered

Table 1 UV thermal denaturation data of DNA-templated autoligation experiments

Entry		Sequences[a]		Control[b]	T_m/°C[c]		
					pH 7.5	pH 8.5	pH 9.5
1	ODN**C**	3′-TTTTTTT		14.8	–	–	–
2	ODN**1**		**1**GCTGCC-5′	38.7	–	–	–
3[d]	ODN**B**/ODN**1**	3′-TTTTTTT^{bn}	**1**GCTGCC-5′	14.8	20.9	27.9	30.8
4[d]	ODN**B**/ODN**2**	3′-TTTTTTT^{bn}	**2**GCTGCC-5′	16.8	13.7	13.6	13.4
5[d]	ODN**B**/ODN**3**	3′-TTTTTTT^{bn}	**3**GCTGCC-5′	12.1	11.0	12.1	16.1
6[d]	ODN**B**/ODN**4**	3′-TTTTTTT^{bn}	**4**GCTGCC-5′	13.5	12.1	12.4	12.3
7[d]	ODN**B**/ODN**5**	3′-TTTTTTT^{bn}	**5**GCTGCC-5′	14.7	13.4	13.9	13.7
8[d]	ODN**B**/ODN**7b**	3′-TTTTTTT^{bn}	**7**GCTGCC-5′	16.0	13.0	12.9	10.9

Template ODN**D** is 5′-d(AAAAAAAACGACGG)-3′

[a] T^{bn} refers to boronothymidine

[b] T_m values indicated refer to the control ODN**C**/ODN**X** at pH 7.5. No major variation could be observed at higher pHs

[c] Melting temperatures refer to the melting of the corresponding sequence(s) with ODN**D** and were obtained from the maxima of the first derivative of the melting curve (A260 vs. temperature) recorded in a buffer containing 0.5 M NaCl and 10 mM of sodium cacodylate, DNA concentration 3 μM of each strand. Curve fit data were averaged from fits of three denaturation curves

[d] T_m values indicated refer only to the lowest temperature-dependent transition

base-pairing rules are still obeyed with UNA monomers [40]. Thus, although UNA contains a 2′-hydroxyl group, it appears that its highly flexible nature prevents the formation of a stable boronate linkage. This observation could also be explained in terms of the higher energy required for the system to generate an eight-membered ring. ODN**3**, which carries an added methyl group at the 2′ position, induced a slight destabilization at pH = 7.5 (T_m = 11.0 vs. 12.1 °C, Table 1, entry 5) and proved inefficient for ligation of the probes at pH = 8.5. However, the stabilization observed at pH = 9.5, although modest, demonstrates that the ligation could proceed and provide information about the optimal structural requirements. As we previously noted, an RNA-like conformation on the ribonucleoside partner is preferred to promote an efficient autoligation process [26]. The estimated percentage of the north (C3′ endo) conformation in 2′-C-methyl uridine is 90 % (measured by ^{1}H NMR) [41]. Thus, despite the preorganization of the cis-diol motif in ODN**3**, neither the trigonal nor the tetrahedral complex is particularly stable. Molecular dynamics simulations have shown that tetrahedral internucleosidic linkages almost exclusively prefer a single conformer (structure **A**, Fig. 3) [27]. It is thus possible that the addition of a methyl group at the 2′-position creates an

unavoidable axial interaction that results in significant complex destabilization with the adjacent ribose as represented in structure **B** (Fig. 3), thus suggesting that geometric and steric factors appear to exert significant control of the complex stability.

We next shifted our attention to examine the potential ability of the templated system to generate oxazaborolidine linkages with ODN**4** and ODN**5**, which exist in 25 and 100 % C3′-endo conformations, respectively [42, 43]. While it is true that most oxazaborolidines are known to be sensitive to water, studies describing the formation of *sp*3 hybridized boroxazolidines in the presence of water have been reported [44, 45]. Considering that upon hybridization the template significantly increases the effective molarity of the reactants, we anticipated the possibility of generating stable oxazaborolidine linkages. Unfortunately, neither ODN**4** nor ODN**5** could mediate such linkages (Table 1, entries 6 and 7).

In the case of ODN**6** and ODN**7a**, no transition could be observed whatever the pH because of the destabilization induced by the removal of one base pair (data not shown). The proper number of bases if necessary is nevertheless not sufficient to induce a boronate linkage with the glyceryl partner, as can be seen Table 1, entry 8. These results are very useful for evaluating the reaction scope of the DNA-templated autoligation system and highlight the importance of structural mimicry of the DNA backbone.

RNA-templated autoligation experiments performed in the presence ORN**R** confirmed the results obtained with its DNA counterpart. Indeed, ODN**1** and ODN**3** were the only sequences able to induce a boronate junction. Compared to DNA, the RNA template displayed higher stabilizations against the nicked system at pH = 9.5 with ODN**1** (T_m = 30.8 vs. 14.8 °C, ΔT_m = 17.9 °C for ODN**D** and T_m = 32.9 vs. 15.0 °C, ΔT_m = 16.0 °C for ORN**R**). However, the pH dependency decreased slightly (T_m = 30.8 vs. 20.9 °C, ΔT_m = 11.4 °C for ODN**D** and T_m = 32.9 vs. 21.5 °C, ΔT_m = 9.9 °C for ORN**R**). Although less marked, an identical trend was observed with ODN**3**. Its RNA-like structure allows a slight stabilization of the resulting duplex at pH = 7.5 and a minor increased pH dependency (T_m = 16.1 vs. 11.0 °C, ΔT_m = 5.1 °C for ODN**D** and T_m = 17.3 vs. 14.0 °C, ΔT_m = 4.0 °C for ORN**R**), but inevitable steric congestion does not permit a higher degree of complex stability. As was the case in the DNA-templated experiments, all other modifications were unable to promote ligated duplexes (Table 2).

Finally, ODN**1** and ODN**3** were evaluated in the presence of cyanide ions as an external stimulus to uphold stable cyanoboronate junctions at pH = 7.5. Experiments performed in the presence of NaCN (3 mM) at pH = 7.5 on ODN**1** and ODN**3** confirmed that a high level of stabilization could be achieved at neutral pH both in DNA- and RNA-templated systems (Table 3).

In summary, the data presented in this article reveal that geometric and steric structural features are the prevailing factors that control the stability of boronate internucleosidic linkages. If more stable complexes inside a double helix are to be created, these factors will require close attention, but at this stage natural ribonucleotides appear to be the most effective partners. A second feature is the destabilizing role of added diol linkers, emphasizing the importance of adjusted base pairs. These findings complement our earlier studies devoted to the assembly of stimuli-responsive architectures and highlight the selective association of natural ribonucleotidic partners over modified ones.

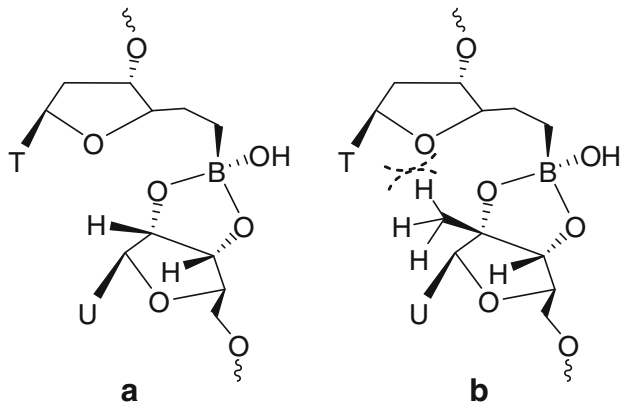

Fig. 3 Conformational representations of the *sp*3 linkages with ODN**1** (**a**) and ODN**3** (**b**)

Experimental

Reactions were conducted in oven-dried glassware. All reagents were purchased from Aldrich or local suppliers and used without purification. All reactions were monitored by TLC, and visualization was effected with UV and/or by developing in vanillin. Chromatography refers to open column chromatography on silica gel (Merck, 40–63 μm). NMR spectra were recorded on a Bruker DRX-300 MHz spectrometer at 300 MHz (^{1}H) and 75 MHz (^{13}C) at 298 K. Chemical shifts are reported in ppm relative to the solvent residual peak $CDCl_3$ as internal standard (^{1}H and ^{13}C). Data for ^{1}H are reported as follows: chemical shift, multiplicity (s = singlet, d = doublet, t = triplet, m = multiplet), coupling constants (*J*) in Hz, and integration. Oligonucleotides were synthesized on a 1-μmol scale using standard phosphoramidite coupling chemistry and analyzed by RP-HPLC (Dionex Ultimate 3000) with a Nucleodur 100-3 C18 column (75 × 4.6 mm; Macherey–Nagel) and by MALDI-TOF MS (Voyager Perseptive Biosystems) using trihydroxyacetophenone (THAP) or

Table 2 UV thermal denaturation data of RNA-templated autoligation experiments

Entry		Sequences[a]		Control[b]	T_m/°C[c]		
					pH 7.5	pH 8.5	pH 9.5
1	ODN**C**	3′-TTTTTTT			–	–	–
2	ODN**1**		**1**GCTGCC-5′		–	–	–
3[d]	ODN**B**/ODN**1**	3′-TTTTTTT^{bn}	**1**GCTGCC-5′	15.0	21.5	31.9	32.9
4[d]	ODN**B**/ODN**2**	3′-TTTTTTT^{bn}	**2**GCTGCC-5′	15.0	15.0	15.0	14.0
5[d]	ODN**B**/ODN**3**	3′-TTTTTTT^{bn}	**3**GCTGCC-5′	12.3	14.0	15.1	17.3
6[d]	ODN**B**/ODN**4**	3′-TTTTTTT^{bn}	**4**GCTGCC-5′	13.0	12.0	11.9	7.7
7[d]	ODN**B**/ODN**5**	3′-TTTTTTT^{bn}	**5**GCTGCC-5′	14.9	14.9	10.9	10.9
8[d]	ODN**B**/ODN**7b**	3′-TTTTTTT^{bn}	**7**GCTGCC-5′	17.0	12.1	12.1	11.1

Template ORN**R** is 5′-r(AAAAAAAACGACGG)-3′

[a] T^{bn} refers to boronothymidine

[b] T_m values indicated refer to the control ODN**C**/ODN**X** at pH 7.5. No major variation could be observed at higher pHs

[c] Melting temperatures refer to the melting of the corresponding sequence(s) with ORN**R** and are obtained from the maxima of the first derivative of the melting curve (A260 vs. temperature) recorded in a buffer containing 0.5 M NaCl and 10 mM of sodium cacodylate, DNA concentration 3 μM of each strand. Curve fit data were averaged from fits of three denaturation curves

[d] T_m values indicated refer only to the lowest temperature-dependent transition

Table 3 Effect of cyanide ions on the UV thermal denaturation data of DNA-template[a] and RNA-template[b] autoligation experiments

Entry		Sequences[c]		T_m/°C[d]
1[a,e]	ODN**B**/ODN**1**	3′-TTTTTTT^{bn}	**1**GCTGCC-5′	24.9
2[b,e]	ODN**B**/ODN**1**	3′-TTTTTTT^{bn}	**1**GCTGCC-5′	27.9
3[a,e]	ODN**B**/ODN**3**	3′-TTTTTTT^{bn}	**3**GCTGCC-5′	18.9
4[b,e]	ODN**B**/ODN**3**	3′-TTTTTTT^{bn}	**3**GCTGCC-5′	19.7

[a] Template ODN**D** is 5′-d(AAAAAAAACGACGG)-3′

[b] Template ORN**R** is 5′-r(AAAAAAAACGACGG)-3′

[c] T^{bn} refers to boronothymidine

[d] Melting temperatures refer to the melting of the corresponding sequence(s) with ODN**D** or ODN**R** and are obtained from the maxima of the first derivative of the melting curve (A260 vs. temperature) recorded in a buffer containing 3 mM NaCN, 0.5 M NaCl, 10 mM of sodium cacodylate, and DNA/RNA concentration 3 μM of each strand. Curve fit data were averaged from fits of three denaturation curves

[e] T_m values indicated refer only to the lowest temperature-dependent transition

3-hydroxypiconilic acid (HPA) as matrix and ammonium citrate as co-matrix. The boronothymidine phosphoramidite was synthesized as previously described [27].

2′-Methyl-5′-O-(4,4′-dimethoxytrityl)uridine ($C_{31}H_{32}N_2O_8$)

After 4 coevaporations with anhydrous pyridine, 105 mg 2′-methyluridine (0.41 mmol) was dissolved in 2.5 cm^3 anhydrous pyridine and mixed with 167 mg dimethoxytrityl chloride (0.49 mmol) under argon atmosphere for 45 min. The reaction was quenched by addition of 3 cm^3 water, and the mixture was extracted with ethyl acetate (2 × 5 cm^3). The organic layer was washed with a saturated solution of sodium hydrogen carbonate (3 × 5 cm^3), dried over Na_2SO_4, and concentrated. The crude product was purified by column chromatography on silica with 50–80 % ethyl acetate in cyclohexane to yield a yellow foam (206 mg, 90 %). ^{1}H NMR (400 MHz, $CDCl_3$): $\delta = 10.58$ (s, 1H), 8.27 (d, $J = 8.1$ Hz, 1H), 7.42–7.25 (m, 10H), 6.87–6.85 (m, 4H), 6.07 (s, 1H), 5.25 (d, $J = 8.3$ Hz, 1H), 4.02–4.15 (m, 2H), 3.79 (s, 6H), 3.58 (s, 2H), 3.15 (d, $J = 9.4$ Hz, 1H), 1.34 (s, 3H) ppm; ^{13}C NMR (100 MHz, $CDCl_3$): $\delta = 163.8, 158.7, 151.2, 144.5, 140.7, 135.3, 135.1, 130.3, 130.1, 129.2, 128.2, 128.0, 127.2, 113.3, 102.6, 92.0, 87.1, 82.2, 78.7, 73.2, 55.2$ ppm.

CPG-succinyl-2′-C-methyluridine

Succinyl-CPG resin (250 mg), 28 mg 2′Me rU (0.05 mmol), 3 mg 4-DMAP (0.025 mmol), 20 mm^3 Et_3N, and 96 mg EDC·HCl (0.5 mmol) were mixed in 3 cm^3 of anhydrous pyridine in a sealed tube and shaken overnight. The reaction mixture was filtrated, and the resin was washed with

dichloromethane and dried under reduced pressure. In a sealed tube, the resin was shaken for 1 h with 1 cm^3 acetic anhydride and 1 cm^3 methylimidazole. After filtration, the resin was washed with dichloromethane and dried under reduced pressure. The obtained loading was 39.7 μmol g^{-1}.

Acknowledgments We thank the Agence Nationale de la Recherche (ANR PRODYGY-11-JS07-005-01) and the Région Languedoc-Roussillon (Programme Chercheur d'Avenir) for providing financial support for our research.

References

1. Eigen M (1971) Naturwissenschaften 58:465
2. Eigen M, Schuster P (1977) Naturwissenschaften 64:541
3. Westheimer FH (1987) Science 235:1173
4. Orgel LE (1995) Acc Chem Res 28:109
5. Orgel LE (1998) Trends Biochem Sci 23:491
6. Orgel LE (2000) Proc Natl Acad Sci USA 97:12503
7. Miyakawa S, Joshi PC, Gaffey MJ, Gonzalez-Toril E, Hyland C, Ross T, Rybij K, Ferris JP (2006) Origins Life Evol B 36:343
8. Dolinnaya NG, Sokolova NI, Ashirbekova DT, Shabarova ZA (1991) Nucleic Acids Res 19:3067
9. Herrlein MK, Nelson JS, Letsinger RL (1995) J Am Chem Soc 117:10151
10. Rohatgi R, Bartel DP, Szostak JW (1996) J Am Chem Soc 118:3332
11. Xu Y, Kool ET (2000) J Am Chem Soc 122:9040
12. Xu YZ, Kool ET (1999) Nucleic Acids Res 27:875
13. Vonkiedrowski G (1986) Angew Chem Int Ed 25:932
14. Kleiner RE, Brudno Y, Birnbaum ME, Liu DR (2008) J Am Chem Soc 130:4646
15. Mattes A, Seitz O (2001) Chem Commun 37:2050
16. Summerer D, Marx A (2002) Angew Chem Int Ed 41:89
17. Peng XH, Li H, Seidman M (2010) Eur J Org Chem, p 4194
18. El-Sagheer AH, Brown T (2011) Chem Commun 47:12057
19. Lehn JM (2007) Chem Soc Rev 36:151
20. Engelhart AE, Hud NV (2010) Cold Spring Harbor Perspect Biol 2:a002196
21. Li ZY, Zhang ZYJ, Knipe R, Lynn DG (2002) J Am Chem Soc 124:746
22. Engelhart AE, Cafferty BJ, Okafor CD, Chen MC, Williams LD, Lynn DG, Hud NV (2012) Chem Bio Chem 13:1121
23. Bean HD, Anet FAL, Gould IR, Hud NV (2006) Origins Life Evol B 36:39
24. Ura Y, Beierle JM, Leman LJ, Orgel LE, Ghadiri MR (2009) Science 325:73
25. Luvino D, Baraguey C, Smietana M, Vasseur JJ (2008) Chem Commun 44:2352
26. Martin AR, Mohanan K, Luvino D, Floquet N, Baraguey C, Smietana M, Vasseur JJ (2009) Org Biomol Chem 7:4369
27. Martin AR, Barvik I, Luvino D, Smietana M, Vasseur JJ (2011) Angew Chem Int Ed 50:4193
28. Martin AR, Vasseur JJ, Smietana M (2012) Pure Appl Chem 84:1659
29. Jin S, Cheng Y, Reid S, Li M, Wang B (2010) Med Res Rev 30:171
30. Nishiyabu R, Kubo Y, James TD, Fossey JS (2011) Chem Commun 47:1106
31. Hall DG (2005) Boronic acids. Preparation and applications in organic synthesis and medicine, Wiley-VCH, Weinheim
32. Springsteen G, Wang BH (2002) Tetrahedron 58:5291
33. DiCesare N, Lakowicz JR (2002) Anal Biochem 301:111
34. Galbraith E, James TD (2010) Chem Soc Rev 39:3831
35. Xu Z, Kim SK, Han SJ, Lee C, Kociok-Kohn G, James TD, Yoon J (2009) Eur J Org Chem, p 3058
36. Badugu R, Lakowicz JR, Geddes CD (2005) Dyes Pigm 64:49
37. Luvino D, Smietana M, Vasseur JJ (2006) Tetrahedron Lett 47:9253
38. Luvino D, Gasparutto D, Reynaud S, Smietana M, Vasseur JJ (2008) Tetrahedron Lett 49:6075
39. Yan J, Springsteen G, Deeter S, Wang B (2004) Tetrahedron 60:11205
40. Pasternak A, Wengel J (2011) Org Biomol Chem 9:3591
41. Beigelman LN, Ermolinsky BS, Gurskaya GV, Tsapkina EN, Karpeisky MY, Mikhailov SN (1987) Carbohydr Res 166:219
42. Guschlbauer W, Jankowski K (1980) Nucleic Acids Res 8:1421
43. Campbell MA, Wengel J (2011) Chem Soc Rev 40:5680
44. Futatsugi K, Yamamoto H (2005) Angew Chem Int Ed 44:1484
45. Rico AR, Tlahuextl M, Flores-Parra A, Contreras R (1999) J Organomet Chem 581:122